

NOTICE

**CERTAIN DATA
CONTAINED IN THIS
DOCUMENT MAY BE
DIFFICULT TO READ
IN MICROFICHE
PRODUCTS.**

DEC 13 1991

Los Alamos National Laboratory is operated by the University of California for the United States Department of Energy under contract W-7405-ENG-36

TITLE: An Efficient, Three Dimensional, Fully-Coupled
Hydro-Thermo-Mechanical Simulator: FEHMS

AUTHOR(S): Sharad Kelkar, EES-4
George A. Zivoloski, EES-5

SUBMITTED TO: 11th SPE Symposium on Reservoir Simulation
February 11-13, 1991, Anaheim, California

DISCLAIMER

This report was prepared as an account of work sponsored by an agency of the United States Government. Neither the United States Government nor any agency thereof, nor any of their employees, makes any warranty, express or implied, or assumes any legal liability or responsibility for the accuracy, completeness, or usefulness of any information, apparatus, product, or process disclosed, or represents that its use would not infringe privately owned rights. Reference herein to any specific commercial product, process, or service by trade name, trademark, manufacturer, or otherwise does not necessarily constitute or imply its endorsement, recommendation, or favoring by the United States Government or any agency thereof. The views and opinions of authors expressed herein do not necessarily state or reflect those of the United States Government or any agency thereof.

By acceptance of this article, the publisher recognizes that the U.S. Government retains a nonexclusive, royalty-free license to publish or reproduce the published form of this contribution, or to allow others to do so, for U.S. Government purposes.

The Los Alamos National Laboratory requests that the publisher identify this article as work performed under the auspices of the U.S. Department of Energy

Los Alamos Los Alamos National Laboratory
Los Alamos, New Mexico 87545

An Efficient, Three Dimensional, Fully-Coupled Hydro-Thermo-Mechanical Simulator: FEHMS

Sharad Kelkar and George Zyvoloski

Los Alamos National Laboratory, Los Alamos, New Mexico, USA

ABSTRACT

Hydro-thermo-mechanical effects in fractured rocks are important in many oilfield processes. Modeling these effects is made difficult by the fact that the governing equations are nonlinear and coupled, and the problems to be solved are three dimensional. In this paper we describe a numerical code developed for this purpose. The code is finite element based to allow for complicated geometries, and the time differencing is implicit, allowing for large time steps. The use of state-of-the-art equation solvers has resulted in a practical code. An example is presented to demonstrate the effects of matrix expansion, due to pore pressure and heating, on fracture opening due to fluid injection, and induced stress changes at a distant well bore.

INTRODUCTION

Oil production is almost always enhanced by hydraulic fracturing or injection strategies. Stress changes during fracturing operations are directly responsible for the permeability increase observed in such operations. Here the effective stress is decreased by increasing the fluid pressure until induced and/or pre-existing fractures are opened and propped. Pore pressure effects also cause subsidence in oil and gas reservoirs along the Gulf coast. Temperature differences can also affect stresses in a reservoir. In the North Sea, cold sea water is injected into heterogeneous formations with temperature differences of up to 100°C. This causes rock contraction which in turn causes permeability increases. Steam injection is used commonly in limestone formations. Here large temperature differences also occur, but the rock now expands causing a permeability decrease. This process is depicted in Fig. 1. Coupled hydro-thermal-mechanical processes are also important in other engineering applications such as geothermal energy production, underground waste storage, and

in understanding many fundamental geophysical phenomena. These phenomena include transport of magma through the crust, and the migration of oil.

Due to the importance of the coupled processes, considerable effort has been devoted to solving the mathematical equations representing these processes. The analytical work in this area has been, of necessity, limited to the study of one or two of the hydraulic, thermal, and deformational processes (e.g., Rice and Cleary, 1976, Palciauskas and Domenico, 1989, Perkins and Kern, 1961, Elsworth, 1989). This is due to the fact that the equations involved are coupled and nonlinear. Solutions have also been obtained using semi-analytical techniques, where simplifying assumptions and similarity arguments are used to reduce the set of coupled, nonlinear, multi-dimensional partial differential equations to a more manageable ordinary differential equation (e.g., Wijesinghe, 1986). These studies are extremely valuable in providing an insight into the physics of the coupled phenomena and in setting the stage for more involved numerical, computer based solution techniques.

Over the past few decades several numerical codes have been developed to model various aspects of the coupled hydro-thermo-mechanical processes. Use has been made of different forms and combinations of finite difference (e.g., Hopkirk and Rybach, 1989, Hart and St. John, 1986), finite element (e.g., Noorishad et al., 1982, Ohnishi et al., 1985) and discrete element (e.g., Cundall, 1985) techniques to discretize the spatial domain of the problem for computational purposes. In most of these approaches, the time dependence of the equations is solved explicitly, typically using successive substitution to solve at least some of the several equations at a given time and then marching explicitly forward in time. This procedure has the advantage of simplicity and of not having to deal with a large number of nonlinear, simultaneous equations, but suffers from having to use small time steps to get stable solutions, making large simulations, over thousands of years, impractical.

In order to avoid these difficulties, work is under way to develop a robust and flexible numerical code, FEHMS (Finite Element Heat Mass Stress), at Los Alamos National Laboratory. A fully implicit, coupled formulation is used to allow for large time steps. This approach requires the solution of nonlinear, coupled discretized equations at each time step. The Newton-Raphson technique is used to handle nonlinearities. The resulting matrix equations are solved using an ortho-minimization technique accelerated with incomplete factorization (Zyvoloski, 1986). The code is finite element based in order to allow for complicated geometries, however, the technique is modified to facilitate upwinding. In this paper we describe the mathematical model used to represent the coupled processes in a fractured geological medium. A description of the code and the numerical techniques is also given. The code is then applied to the problem of non-isothermal fluid injection into a pre-existing fracture including the poroelastic and thermal effects within the surrounding matrix.

MATHEMATICAL MODEL

Fluid flow is modeled using the mass balance within a compressible medium combined with the Darcy law for flux (Earlaugher, 1977). The permeability and porosity of the matrix is allowed to vary as a known function of the local fluid pressure. The permeability of the fractures, on the other hand, is expressed as a power law function of the fracture aperture (Tsang and Witherspoon, 1981), calculated from the displacement equations. Conservation of mass of the pore fluid is expressed by

$$\frac{\partial A_m}{\partial t} + \nabla \cdot f_m + q_m = 0,$$

where the mass of fluid per unit volume is

$$A_m = \phi \rho$$

and the mass flux is

$$f_m = \rho V$$

where ϕ is the porosity of the matrix (void volume/total volume), V is the fluid velocity, ρ is the fluid density, and q_m is the mass source. This equation is augmented with Darcy's law for single phase flow through a porous medium

$$V = -\frac{k}{\mu} \nabla P$$

where k is the permeability, μ is the fluid viscosity, and P is the fluid pressure.

The fracture permeability k_f is given by

$$k_f = f * w^n$$

where f is a numerical factor, w is the aperture and n is the power law exponent. In the examples presented here n is taken to be 2.0

The energy balance is performed for the rock-fluid mixture assuming that the rock and fluid are in equilibrium with each other at every point, given by

$$\frac{\partial A_e}{\partial t} + \nabla \cdot f_e + q_e = 0$$

where the energy per unit volume is

$$A_e = (1 - \phi)\rho_r U_r + \phi \rho U$$

and the energy flux vector is

$$f_e = \rho h V - K \nabla T$$

Here U_r is the specific internal energy of the rock, U is the specific internal energy of the fluid, h is the specific enthalpy of the fluid, T is the temperature, q_e is the energy source, and K is the bulk thermal conductivity.

Solid displacements are calculated using static stress balance with Biot's poroelastic equations for small displacements (Biot, 1941). Linear thermoelasticity (Timoshenko and Goodier, 1951) is used to include thermal expansion/contraction effects. The static form of the force balance inside the porous solid leads to

$$\frac{\partial \sigma_{ij}}{\partial x_j} + b_i = 0$$

where b_i is the body force, i, j , and k are indices in cyclic order for a Cartesian coordinate system, and σ_{ij} are the components of the stress tensor in the porous solid. For points on the fracture face, an additional external force is present due to the fluid pressure within the fracture. Using the theory of linear poroelasticity for small strains, these are related to the strain tensor, ϵ_{ij} , by

$$\epsilon_{ij} = \frac{\sigma_{ij}}{E} - \frac{\nu}{E}(\sigma_{jj} + \sigma_{kk}) - \frac{\Delta P}{3H} + \alpha \Delta T$$

for the diagonal components, where no sum is implied over repeated indices, and the offdiagonal components are given by

$$\epsilon_{ij} = \frac{2(1+\nu)}{E} \sigma_{ij} ,$$

where α is the coefficient of thermal expansion, E is Young's modulus, ν is Poisson's ratio and H is Biot's physical constant.

Hydro-thermal coupling occurs through the pressure and temperature dependence of fluid density, viscosity, and enthalpy and through the convection terms in the energy equation. The mass and energy equations are also affected by pressure and temperature through the dependence of rock porosity and permeability on these quantities as well as on rock displacements. Hydro-mechanical coupling occurs through the strong dependence of fracture porosity and permeability on displacements and through the inclusion of pore pressure terms in Biot's equations. Thermo-mechanical coupling is included through the temperature terms in the thermoelasticity equation and through the dependence of porosity and permeability on displacements in the convection terms in the energy equation.

NUMERICAL PROCEDURES

The space derivatives in the governing equations are discretized using the finite element method with the Galerkin formulation. At present only linear elements are used in the coupled code. The primary dependent variables interpolated on each element are the fluid pressure, P , fluid temperature, T and the three solid displacements, U, V , and W in the x, y , and z directions respectively. The stress equations are formulated with displacements as unknowns. Although the code is finite element based, all the variables and material properties are defined at the nodes. The nonlinear material properties are factored out of the equation coefficients and interpolated between the nodes, evaluated at each iteration. This results in a considerable computational saving as the shape function integrals need to be evaluated only once at the start of the program. This approximation is consistent for small strains. Permeabilities in the flux terms are harmonically averaged. The shape functions are evaluated with the use of either Lobatto or Gauss quadrature. Lobatto quadrature has the same formal accuracy as the Gauss quadrature while yielding considerably fewer nonzero matrix elements. It has been found to work well in heat-flow problems but leads to inaccurate results for the displacement equations.

The nodes that form the fracture are treated differently than those in the rock matrix. Full upwinding (donor cell) is used in the fluid flow and energy transport equations for the fracture nodes. This is facilitated by using a linear combination of the permeability along the fracture instead of harmonic weighting. The permeability perpendicular to the fracture is harmonically averaged.

Time discretization is accomplished by using the first order, backward Euler method. This is a fully implicit scheme where all functional dependencies are evaluated at the new time step. This leads to a set of nonlinear, coupled algebraic

equations that have to be solved at each time step. The Newton-Raphson technique is used to solve these nonlinear equations. The full Jacobian is formed at each iteration. Use of nonlinear polynomial fits to thermodynamic functions has resulted in considerable computational savings. The resultant linear matrix equations are solved by factoring the coefficient matrix. The matrix solution is performed using an iterative ortho-minimization technique accelerated with incomplete factorization. The Newton-Raphson scheme is iterated until the norm of the residuals of the balance equations decreases by a prescribed factor.

SOLUTION STRATEGY

The computational efficiency of the code relies on the strategies involved in solving the linear set of equations at each Newton-Raphson iteration for the five degrees of freedom. In this section we describe the Preconditioned Conjugate Gradient Solver employed and some of the variants we are investigating. Table 1 shows the form of the linear equation set which must be solved at each Newton-Raphson iteration. We employ incomplete factorization (ILU) as the preconditioner and GMRES as the acceleration scheme. ILU methodology is described well by Behie and Vinsome (1982). A description of GMRES may be found in Saad and Schultz (1986). The $5n$ by $5n$ system is solved in block form using a pointer system allowing for a variable number of neighbors among the nodes. By solving the system in block form the pointer array need only be the same size as one for an n by n system. In what follows, this method is referred to as the Fully Implied Method (FIM). The solver employed also allows arbitrary levels of fill. That is, the preconditioner may be ILU(n), where n is arbitrary. The acceleration method is a multiple degree of freedom GMRES algorithm. The approximate storage requirements for the preconditioner and the acceleration algorithm are given in Table 2.

The coupled system with the stress equations can be stiff and difficult to solve. It often requires ILU(3) to converge properly, this in turn can require large storage requirements for FIM for even modest sized 3-d problems. This has motivated us to investigate reduced degree of freedom techniques (RDOF). The RDOF method (Zyvoloski (1988), Bullivant and Zyvoloski (1990)) applied here consists of modifying the 5 dof system shown in Table 2 to a 3 dof system. We do this by neglecting the off diagonal derivatives with respect to the "x" and "y" displacements. Thus the submatrices A_{4i} and $A_{5i}, i=1,5$ in Table 2 become diagonal. With these assumptions the degree of freedom of the system may be reduced as follows.

The equation for the 5th variable may be written

$$A_{51}x_1 + A_{52}x_2 + A_{53}x_3 + A_{54}x_4 + A_{55}x_5 = -R_5 \quad (1)$$

$$x_5 = A_{55}^{-1} \left[-R_5 - A_{51}x_1 - A_{52}x_2 - A_{53}x_3 - A_{54}x_4 \right] \quad (2)$$

where the indicated inversion is trivial because A_{55} is diagonal.

Substituting this expression into the equation for the 4th variable and rearranging terms we have

$$\begin{aligned} & \left[A_{41} - A_{45} A_{55}^{-1} A_{51} \right] x_1 + \left[A_{42} - A_{45} A_{55}^{-1} A_{52} \right] x_2 \\ & + \left[A_{43} - A_{45} A_{55}^{-1} A_{53} \right] x_3 + \left[A_{44} - A_{45} A_{55}^{-1} A_{54} \right] x_4 = R'_4 \end{aligned} \quad (3)$$

Setting

$$A'_{4j} = \left[A_{4j} - A_{45} A_{55}^{-1} A_{5j} \right], j = 1, 4 \quad (4)$$

$$R'_4 = R_4 - A_{45} A_{55}^{-1} R_5 \quad (5)$$

we have

$$x_4 = A'^{-1}_{44} \left[-R'_4 - A'_{41} x_1 - A'_{42} x_2 - A'_{43} x_3 \right] \quad (6)$$

where the inversion is trivial because of the diagonal form of A_{44} , A_{45} , A_{55}^{-1} , and R_{54} . Rearranging the order of operations between the 4th and 5th variable we may also obtain

$$x_5 = A'^{-1}_{55} \left[-R'_5 - A'_{51} x_1 - A'_{52} x_2 - A'_{53} x_3 \right] \quad (7)$$

where

$$A'_{5j} = \left[A_{5j} - A_{54} A_{44}^{-1} A_{4j} \right], j = 1, 2, 3, 5 \quad (8)$$

$$R'_5 = \left[R_5 - A_{54} A_{44}^{-1} R_4 \right] \quad (9)$$

Eq. (6) and (7) may be substituted into the equations for the first three variables to eliminate the on x_4 and x_5 . The following $3n$ by $3n$ system is obtained

$$\begin{pmatrix} A'_{11} & A'_{12} & A'_{13} \\ A'_{21} & A'_{22} & A'_{23} \\ A'_{31} & A'_{32} & A'_{33} \end{pmatrix} \begin{pmatrix} x_1 \\ x_2 \\ x_3 \end{pmatrix} = \begin{pmatrix} R'_1 \\ R'_2 \\ R'_3 \end{pmatrix} \quad (10)$$

where

$$\begin{aligned} A'_{ij} &= \left[A_{ij} - A_{i4} A_{44}^{-1} A_{4j} - A_{i5} A_{55}^{-1} A_{5j} \right] \\ R'_i &= R_i - A_{i4} A_{44}^{-1} R_4 - A_{i5} A_{55}^{-1} R_5 \end{aligned} \quad (11)$$

The system of equations (10) is solved by a ILU (n) GMRES based solver (Zyvoloski, Kelkar, and Dash, 1991). The variables x_4 and x_5 are obtained by Eq. (6) and (7). Because of the neglected offdiagonal terms in A_{4j} and A_{5j} , the x_i are approximate. This solution may be improved using several

cycles of SOR coupled iterations with the original matrix. We call this method the Improved Reduced Degree of Freedom (IRDOF). It is described in more detail by Zyvoloski (1988) and Zyvoloski and Bullivant (1990). The storage requirements for the RDOF schemes are given in Table 2.

The above mentioned procedure has not yet been fully implemented in the code FEHMS. In the example calculations that follow, the five degree of freedom ILU(n) GMRES solver described in the first paragraph of this section, is used.

EXAMPLE CALCULATIONS

The three dimensional, multiphase, hydro-thermal parts of the code and the two dimensional uncoupled and one way coupled stress code have been verified previously (Zyvoloski and Kelkar, 1987). In this paper we present results for the case of two-dimensional fluid and heat flow, fully coupled with the one-dimensional deformation of the rock matrix. Although the numerical code being developed is capable of fully three-dimensional simulations, it is desirable to start with simpler problems. Comparison is also made with published semianalytical results as a partial verification of the code.

Description of the example problem: A rectangular block of porous, permeable rock with a fracture running along the lower edge is considered, as shown schematically in Figure 2. The lower left hand node is the injection node. Fluid flow and heat transfer are also allowed into the matrix. Matrix deformation changes the fracture aperture. The physical dimensions of the block are 100 meters along the x-axis with 101 nodes and 10 meters along the y-axis with 11 nodes, resulting in a total of 111 nodes and 1000 elements in the problem. The values of various parameters for the base case are shown in Table 3. These values were selected for testing only and are not meant to represent any particular field example. A fixed time step of 10 seconds was used in most examples, although other runs were made to check the effect of time step on the solution.

Results of the base case run: In this edependenceuid is injected at a constant rate into the fracture and allowed to flow along the fracture but not into the matrix perpendicular to the fracture. Fluid injection temperature is the same as the initial uniform rock temperature. The dependence of the fracture permeability on the aperture is modeled with the cubic law. The aperture at the injection point opens rapidly, its growth slowing down in time as the fluid flows forward and the fracture propagates. The aperture as a function of distance from the injection point at various times is shown in Figure 3.

Effects of matrix flow: The next case shown is similar to the previous one except that fluid flow is allowed into the matrix as well, although the poroelastic expansion of the matrix is suppressed. The results for three different values of rock permeability, 10^{-24} m^2 , 10^{-14} m^2 , and 10^{-12} are shown in Figure 4. As expected, the pressure buildup and hence the aperture of the fracture decreases with increasing matrix permeability. The case of 10^{-12} m^2 is interesting, where the initial fracture permeability equals the matrix permeability. The fluid loss is so high that the fracture does not open much.

Figure 5 shows the effect of increasing the injection rate, a larger fracture aperture results from the higher injection rate.

Effects of matrix expansion: Figures 6 and 7 show the fracture aperture for different values of Biot's physical constant and matrix permeability. The expansion of the rock matrix due to the pore pressure buildup caused by fluid diffusion leads to reduced fracture aperture. As seen in Figures 6 and 7, this effect is more pronounced for higher values of the permeability and of the expansion coefficient.

Effects of thermal expansion: Figure 8 shows the fracture profile at various times for non-isothermal fluid injection allowing for thermal expansion of the rock. The coefficient of thermal expansion used here is two orders of magnitude higher than that expected for real rocks so as to amplify the effect during the small simulation time (0.231 hours) that is considered. Similar effects might be expected in real rocks over larger time spans. An interesting fracture profile results. The aperture increase in the beginning as expected, but as the rock temperature near the injection point builds up, its aperture becomes less than that farther along the fracture due to the greater penetration of the thermal front near the injection point.

Combined hydro-thermal-mechanical problem: Figure 9 shows the fracture aperture profile that resulted from the combined effects of fracture opening, matrix permeation, matrix expansion due to pore pressure, heat convection, thermal diffusion, and thermal expansion of the rock. For comparison, the profile without matrix diffusion and thermal expansion is also shown.

REMARKS

1) Three dimensional examples will be given in the oral presentation.

2) The authors feel that with the incorporation of the IRDOF strategy described above would decrease computer costs by a factor of 2 - 10. This has been observed in applications of the FEHM code on which the code (FEHMS) is based.

2) Fracture zones, rather than individual fractures can be treated efficiently with this code. Here the fracture volume, rather than the total volume is used in the aperture permeability relationship describes in the Model section. We plan on implementing these ideas in the dual porosity version of FEHMS.

3) Shear displacements on fracture faces can be important in coupled problems. We plan to incorporate these in the future.

CONCLUSIONS

A fully implicit 3-D coupled Hydro-thermal-mechanical Model, currently under development at Los Alamos, is capable of solving difficult stress related problems found in reservoirs.

With implementation of adaptive solution strategies, it will be capable of modeling large realistic problems.

ACKNOWLEDGEMENTS

This work was supported by the US Department of Energy under the Yucca Mountain Project at the Los Alamos National Laboratory.

REFERENCES

1. Bear, J., *Dynamics of Fluids in Porous Media*, American Elsevier Publishing Company, New York, New York, 1972.
2. Behie, A., and Vinsome, P. K. W., "Block Iterative Methods for Fully Implicit, Reservoir Simulation, *SPEJ*, pp. 658-666, Oct. 1982.
3. Biot, M.A., "General Theory of Three Dimensional Consolidation," *J. App. Phy.*, Vol. 12, pp 155-164 (1941).
4. Cundall, P.A., "Distinct Element Models of Rock and Soil Structure", in *Analytical and Computational Methods in Engineering Rock Mechanics*, E.T. Brown (ed.), London, Allen and Unwin, Publishers, 1985,
5. Elsworth, D., "Thermal Permeability Enhancement of Blocky Rocks: One-Dimensional Flows", *Int. J. Rock Mech. Min. Sci. & Geomech. Abstr.*, Vol. 26, No. 3/4, pp 329-339 (1989).
6. Hart, R.D., and St. John, C.M., "Formulation of a Fully-Coupled Thermal-Mechanical-Fluid Flow Model For Non-Linear Geologic Systems," *Int. J. Rock Mech. Min. Sci. & Geomech. Abstr.*, Vol.23, No. 3, pp. 213-224, (1986).
7. Hopkirk, R.J., and Rybach, L., "Modeling Pressure Behaviour in Artificially Stimulated Rock Masses-Matching Field Pressure Records," *Int. J. Rock Mech. Min. Sci. & Geomech. Abstr.*, Vol. 26, No. 3/4, pp 341-349 (1989).
8. Noorishad, J., Ayatollahi, M.S. and Witherspoon, P.A., "A Finite Element Method For Coupled Stress and Fluid Flow Analysis in Fractured Rock Masses," *Int. J. Rock Mech. Min. Sci. & Geomech. Abstr.*, Vol. 19, pp 185-193 (1982).
9. Ohnishi, Y., Shibata, H., and Kobayashi, A., "Development of Finite Element Code For Coupled Thermo-Hydro-Mechanical Behavior of Saturated-Unsaturated Medium," International Symposium on Coupled Processes Affecting the Performance of a Nuclear Waste Repository, Lawrence Berkeley Laboratory, Berkeley, California, 1985.
10. Palciauskas, V.V., and Domenico, P.A., "Fluid Pressures in Deforming Porous Rocks," *W.R.R.*, Vol. 25, No. 2, pp 203-213, (1989).
11. Perkins, T.K., and Kern, L.R., "Widths of Hydraulic Fractures," *J. Pet. Tech.*, September 1961, pp 937-948, (1961).

12. Rice, J.R., and Cleary, M.P., "Some Basic Stress Diffusion Solutions For Fluid-Saturated Elastic Porous Media With Compressible Constituents," *Reviews of Geophysics and Space Physics*, Vol. 14, No. 2, pp 227-241, (1976).
13. Saad, Y., and Schultz, M. H., "GMRES: a Generalized Minimal Residual Algorithm for Solving Nonsymmetric Linear Systems," *SIAM, J. Sci. Stat. Comput.*, Vol. 7, pp. 856-869, July (1986).
14. Timoshenko, S., and Goodier, J.N., *Theory of Elasticity*, McGraw- Hill Book Company, Inc., New York:1951.
15. Tsang, Y.W. and Witherspoon, P.A., "Hydromechanical Behavior of a Deformable Rock Fracture Subject to Normal Stress," *J.G.R.*, Vol. 86, No. B10, pp 9287-9298, (1985).
16. Tsang, Y.W., and Mangold, D.C., (eds.), "Panel Report on Coupled Thermo-Mechanical-Hydro-Chemical Processes Associated with a Nuclear Waste Repository," Lawrence Berkeley Laboratory, Berkeley, California, 1984.
17. Wijesinghe, A.M., "A Similarity Solution For Coupled Deformation and Fluid Flow in Discrete Fractures," Second International Radioactive Waste Management Conference, Winnipeg, Canada, 1986.
18. Zyvoloski, G., "Incomplete Factorization for Finite Elements," *International Journal for Numerical Methods in Engineering*, Vol. 23, pp. 1101-1109, (1986).
19. Zyvoloski, G., and Kelkar, S.M., "FEHMS: a Finite Element Heat- Mass-Stress Code For Coupled Geological Processes," YMP Milestone R346 report, Los Alamos National Laboratory, Los Alamos, New Mexico, 1987.

Table 1.
Jacobian Matrix for Coupled Heat, Mass and Stress Problem

$$\begin{pmatrix} A_{11} & A_{12} & A_{13} & A_{14} & A_{15} \\ A_{21} & A_{22} & A_{23} & A_{24} & A_{25} \\ A_{31} & A_{32} & A_{33} & A_{34} & A_{35} \\ A_{41} & A_{42} & A_{43} & A_{44} & A_{45} \\ A_{51} & A_{52} & A_{53} & A_{54} & A_{55} \end{pmatrix} \begin{pmatrix} x_1 \\ x_2 \\ x_3 \\ x_4 \\ x_5 \end{pmatrix} = - \begin{pmatrix} R_1 \\ R_2 \\ R_3 \\ R_4 \\ R_5 \end{pmatrix}$$

1 - Mass, 2 = Heat, 3 = x Stress, 4 = Y Stress, 5 = Z Stress

Table 2. Storage Requirements for the ILU GMRES Solver Used in FEHMS (Excluding the Storage for $Ax = b$)

	Factorization	GMRES
	ILU(1)	
FIM	27 x 25 x N	(North + 1) x 5 x N
IRDOF	27 x 9 x N	(North + 1) x 3 x N
	ILU(2)	
FIM	70 x 25 x N	(North + 1) x 5 x N
IRDOF	70 x 9 x N	

Table 3. Parameter Values for the Base Case Example

Length x	100 m
Length y	10 m
Initial pressure	20 Mpa
Initial temperature	25° C
Injection rate	0.1 kg/s
Injection temperature	20° C
Matrix porosity	0.10
Matrix permeability x direction	10 ⁻²⁴ m ²
Matrix permeability y direction	10 ⁻²⁴ m ²
Initial fracture permeability	10 ⁻¹² m ²
Thermal conductivity	2-7 J/m/K
Young's modulus	10 ³ MPa
Poisson's ratio	0.0
Thermal expansion coefficient	5° 10 ⁻⁵
Pore pressure coefficient	10 ⁻¹⁰ /MPa

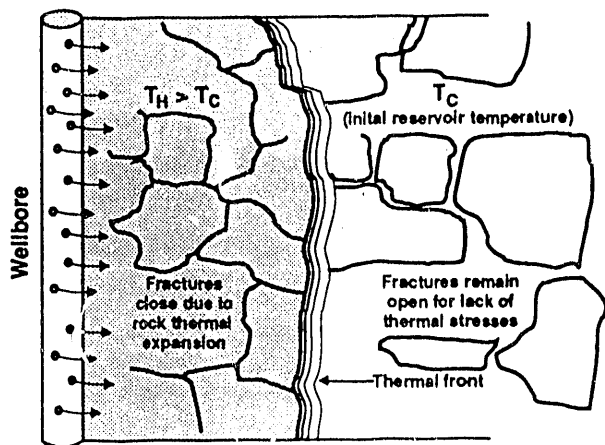


Fig. 1. Temperature differences can cause permeability changes.

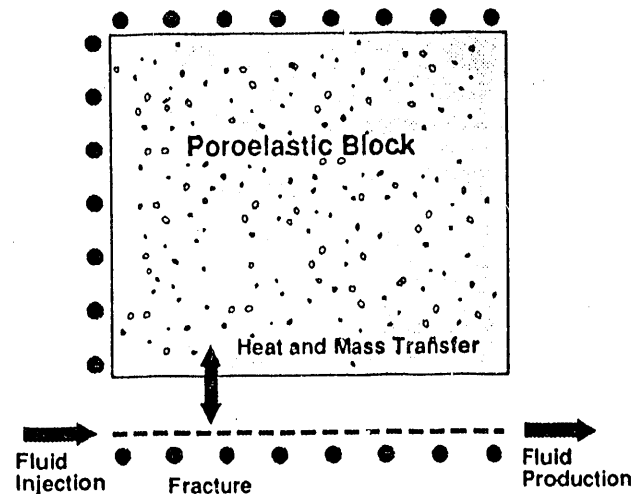


Fig. 2. A schematic of the Coupled fracture flow model.

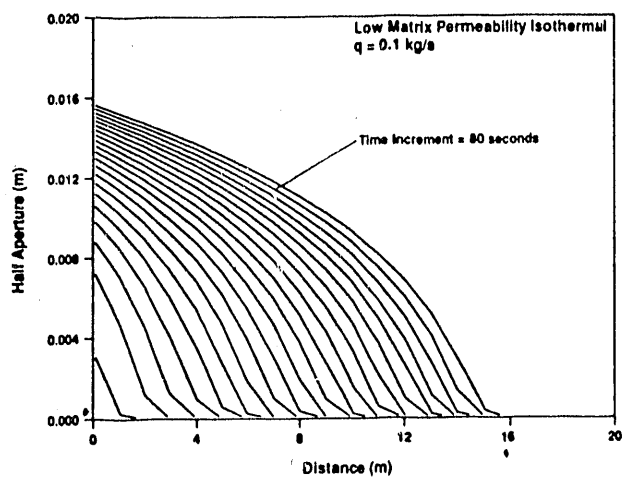


Fig. 3. Fracture opening profile for the base case run.

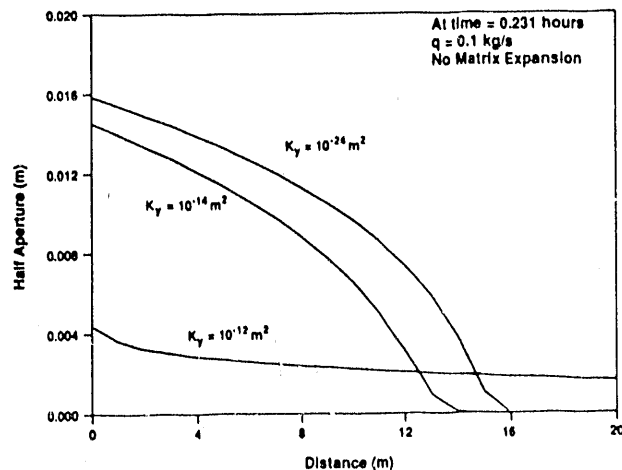


Fig. 4. Fracture opening profile for various values of matrix permeability.

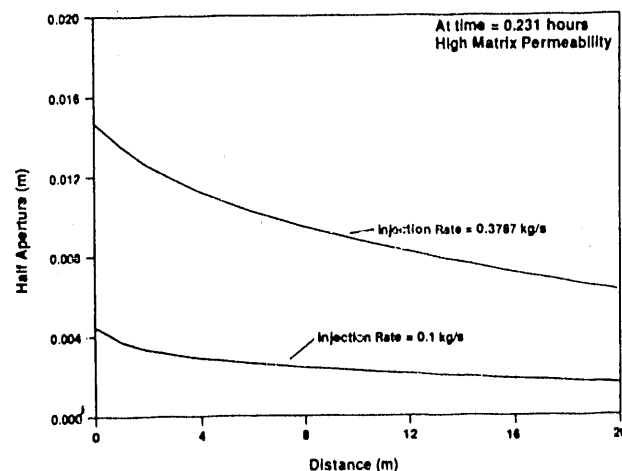


Fig. 5. Effect of injection rate on fracture opening.

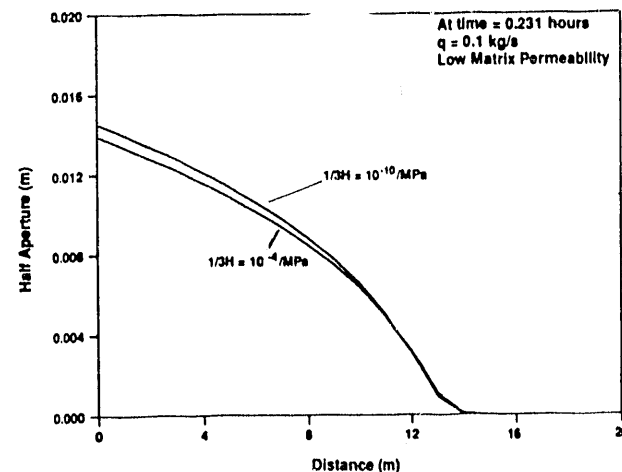


Fig. 6. Effect of Biot's pore pressure coefficient, low matrix permeability case.

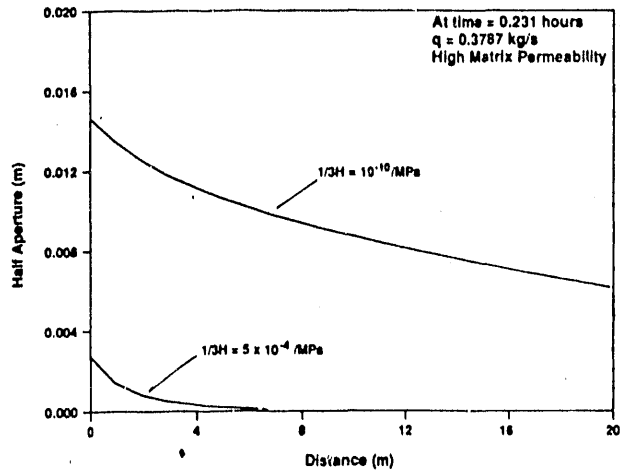


Fig. 7. Effect of Biot's pore pressure coefficient, high matrix permeability case.

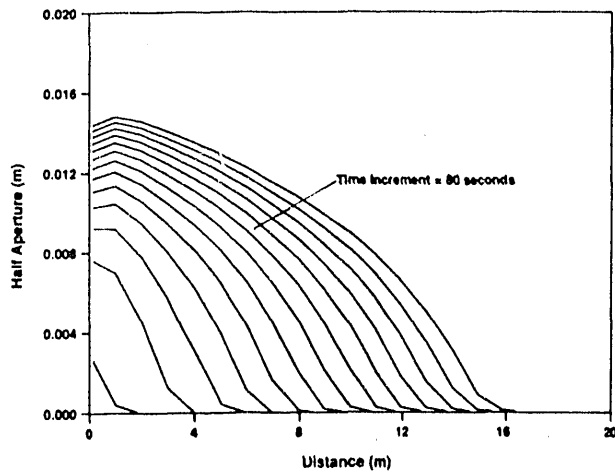


Fig. 8. Fracture opening profile for hot fluid injection including thermal expansion.

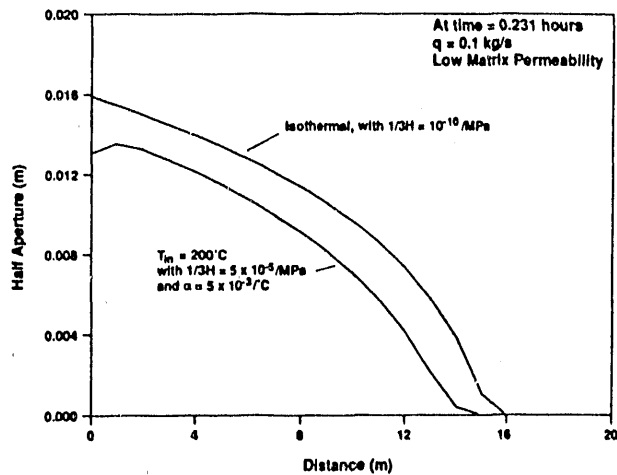


Fig. 9. Comparison of fracture profile for the fully coupled case with the base case.

- END -

DATE FILMED

02 / 27 / 91

